Chattering and Related Behaviour in Impact Oscillators

Chris Budd, Felix Dux

Chattering and related behaviour in impact oscillators

Chris Budd, Felix Dux

One of the most interesting properties of an impacting system is the possibility of an infinite number of impacts occurring in a finite time (such as a ball bouncing to rest on a table). Such behaviour is usually called chatter. In this paper we make a systematic study of chattering behaviour for a periodically forced, single-degree-of-freedom impact oscillator with a restitution law for each impact. We show that chatter can occur for such systems and we compute the sets of initial data which always lead to chatter. We then show how these sets determine the intricate form of the domains of attraction for various types of asymptotic periodic motion. Finally, we deduce the existence of periodic motion which includes repeated chattering behaviour and show how this motion is related to certain types of chaotic behaviour.

1. Introduction

The single degree of freedom impact oscillator comprising a periodically driven oscillating particle, impacting and rebounding against a rigid obstacle has a remarkably rich dynamical structure. Some of the dynamics, such as periodic and certain forms of chaotic behaviour, can be explained by the usual theory of smooth dynamical systems (Thompson & Stewart 1986) but much of it is quite different and due to the essentially discontinuous nature of the impacting process.

Previous papers studying impact oscillators have, in general, either considered solutions which are periodic and repeat after a fixed number of impacts (often one) or are chaotic with an infinite number of essentially random impacts in an infinite time. By restricting the analysis to solutions which repeat after one impact, it is possible to study the bifurcations that these undergo as the parameters in the system are varied. Some examples of these are given in Shaw & Holmes (1983) and Thompson & Stewart (1986) and have subsequently been developed by Whiston (1992), Nordmark (1991) and Budd *et al.* (1993).

In this paper we shall take an opposite approach and examine the dynamical behaviour of those solutions of an impact oscillator which have a very large number or indeed infinite number of impacts in a finite time. One example of this form of behaviour is very familiar: an elastic ball released under gravity from above an obstacle will bounce on the obstacle, acting as a simple impact oscillator. If there is only a small energy loss at each impact then it will bounce a very large number (in an idealized case an infinite number) of times before coming to rest in a finite time. Similar systems arise in many applications in engineering where driven components may collide very frequently against each other or against rigid obstacles, resulting in a high wear rate (Goyda & Teh 1989). Engineers often refer to such behaviour as chatter and throughout this paper we refer to the idealized mathematical description

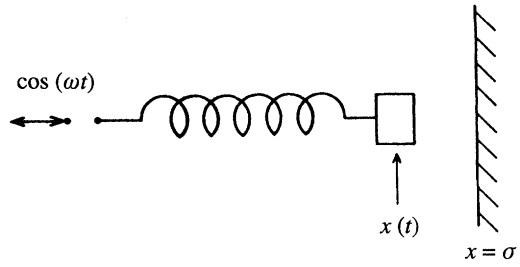

Figure 1. The general form of the impact oscillator.

of this as chatter as well. In this paper we shall examine the dynamical behaviour related to chatter in a mathematical idealization of an impact oscillator. However, we expect that our conclusions are also relevant to more general systems.

A vibrating mechanical component undergoing chatter can be very simply modelled as an oscillating particle which is on a periodically forced spring and is repeatedly impacting with the obstacle. In this case, chatter is likely to occur if the forcing is toward the obstacle but the particle is rebounding away from it. In such circumstances, the particle may still come to rest on the obstacle after a large number of impacts, but due to the forcing it will move away from the obstacle at a later time and the chattering behaviour will then form part of a more complex motion. It is this form of behaviour that we study in this paper. We shall examine other forms of behaviour closely related to chatter, such as cases where there are a large number of impacts but the particle does not come to rest (incomplete chatter), examples where chatter is closely related to chaotic behaviour and the effect that chatter has upon the domains of attraction of periodic solutions. Surprisingly the study of systems with a large number of impacts closely spaced in time is analytically rather simpler than those with fewer, more widely spaced impacts. Indeed we shall see that studying the rather special dynamics of those solutions of impact oscillators with such a large number of impacts can give very valuable insights into the qualitative form of the more general solutions.

To set the scene we now describe the precise form of the idealized impact oscillator we study in this paper. The general such oscillator is illustrated in figure 1 and comprises a particle on a linear spring at position $x(t) \leqslant \sigma$ which is periodically forced at a frequency ω. When $x = \sigma$ the mass impacts with an obstacle and we model this by a simple restitution law so that

$$\mathrm{d}x/\mathrm{d}t\,|_{\text{after collision}} = -r\,\mathrm{d}x/\mathrm{d}t\,|_{\text{before collision}},$$

where $r < 1$ is the coefficient of restitution.

The complete system is then

$$\left.\begin{aligned} \mathrm{d}^2x/\mathrm{d}t^2 + x = f(t), \quad x < \sigma, \\ \dot{x} \to -r\dot{x}, \quad x = \sigma. \end{aligned}\right\} \tag{1}$$

Here various constants such as the mass of the particle, the stiffness of the spring and the magnitude of the forcing have, without loss of generality, been scaled to one (see Budd *et al.* 1993 for the details of this scaling). The forcing function $f(t)$ will be taken to be periodic with frequency ω and to have the property that $f(t) - \sigma$ changes sign. An appropriate such function is

$$f(t) = \cos(\omega t),$$

and for most of this paper we shall assume that $f(t)$ has this form.

The system (1) departs from a physical model in several respects. In particular, we have not considered damping between impacts and have taken very simple models both for the linear motion on the spring and also for the linear form of the impact. These simplifications make the analysis of the behaviour much easier. Certain forms of behaviour will be rather different in the idealized model: for example, during chatter the particle will impact an infinite number of times in the idealized model of an impact but only a large but finite number of times in a more realistic model. Although this does affect the detailed dynamics, the most significant consequence of chattering – that the particle eventually comes to rest – occurs in both models and it is this which has the dominant effect upon the subsequent motion.

The system (1) has three parameters ω, σ and r and its behaviour depends subtly upon the values these take and a review of some of this is given in Shaw & Holmes (1983) and Budd *et al.* (1993).

If the particle is released from the obstacle at a time t and a velocity $\dot{x} = -rv < 0$ then it will in general describe a trajectory $x(t)$ which comprises a sequence of smooth motions between impacts. In figure 2 we illustrate three such motions for the case $\sigma = 0$ and $r = 0.8$ with $\omega = 2.6$, 2.8 and 2.7 respectively. In the first figure, following an initial transient, the motion becomes and stays periodic. In the second the motion is chaotic and following the initial transient is governed by a strange attractor. In the third the particle repeatedly collides with the obstacle and then comes to rest, sticking to it while its acceleration, $f(t) - \sigma$ is positive, and being released from it when its acceleration is first negative.

It is the motion illustrated in figure 2(*c*) which is of most interest to us here and this figure demonstrates the two phenomena of the particle coming to rest after a chattering sequence and then sticking to the obstacle. In figure 3 we give a close up of this part of the motion. A trajectory of the form illustrated in figure 2(*c*) can either be part of a transient or it can in fact repeat and form part of a periodic motion.

There is a closely related phenomenon illustrated in figure 2(*b*) where several low velocity impacts occur close together in an incompletely chattering sequence. These sequences frequently form part of a chaotic motion.

To study the phenomena of chatter, incomplete chatter and sticking it is convenient to describe the system (1) by a map P, and to do this we use the impact map introduced in Whiston (1992) and Shaw & Holmes (1983). To define this map we make two observations of system (1). First the trajectory $x(t)$ of the particle is uniquely defined by the velocity $-rv_0$ at which it leaves the obstacle and the phase ϕ_0 of the time t_0 at which it leaves, where

$$\phi_0 = (t_0) \bmod (2\pi/\omega). \tag{2}$$

Second, as has been shown in Whiston (1992), if v_0 is strictly positive then the trajectory necessarily impacts the obstacle again with velocity $v_1 \geqslant 0$ at a phase ϕ_1. Following the impact the motion continues with initial velocity $-rv_1$.

Thus we may define a map P acting on the phase space $[0, 2\pi/\omega] \times \mathbb{R}^+$ by

$$P(\phi_0, v_0) = (\phi_1, v_1).$$

If $v_1 > 0$, then by simply running time backwards we obtain a unique inverse for P.

As we are interested in examples where the particle comes to rest on the obstacle, we must extend this definition of P to the cases when $v_0 = 0$. If $v_0 = 0$ and $\ddot{x} > 0$ so

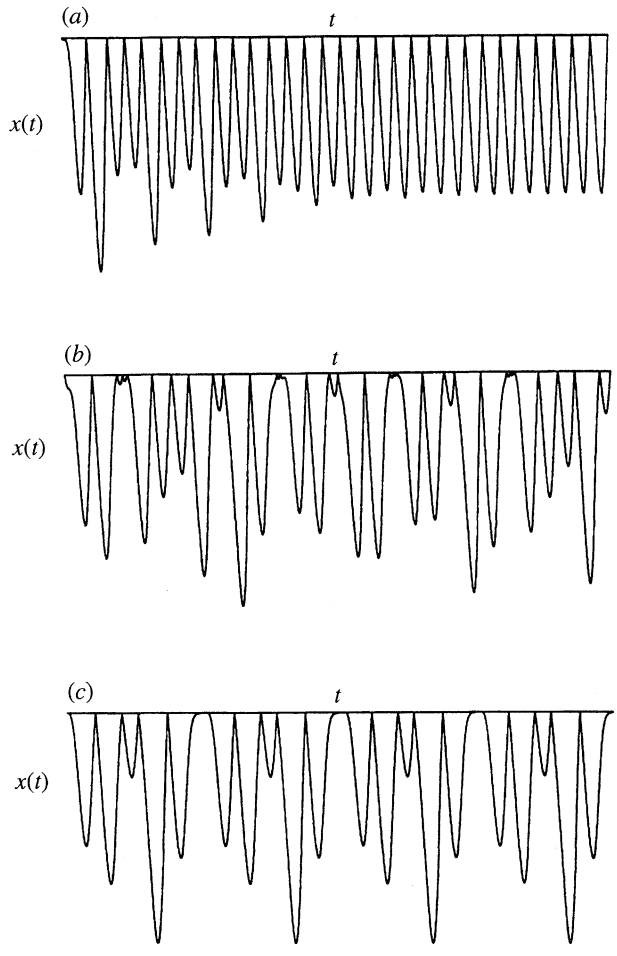

Figure 2. Time series of (*a*) periodic motion arising when $\omega = 2.6$ and $\sigma = 0$; (*b*) chaotic motion arising when $\omega = 2.8$ and $\sigma = 0$; (*c*) chattering motion followed by sticking and subsequent release of the particle arising when $\omega = 2.7$ and $\sigma = 0$.

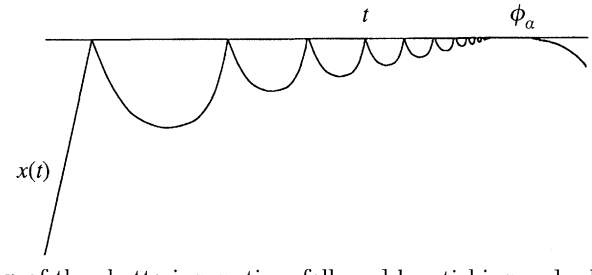

Figure 3. A close up of the chattering motion, followed by sticking and release at the time ϕ_α.

that $f(\phi_0) - \sigma > 0$ then the particle remains stuck to the obstacle until the first point $\phi_\alpha > 0$ at which

$$f(\phi_\alpha) - \sigma = 0,$$

where we assume that $f(t)$ is such that this point occurs. The set of values of ϕ for

which $\ddot{x}$ is positive when $x = \sigma$ is termed by Whiston (1992) the *sticking region* of the map P and we shall assume that this is given by

$$I \equiv [\phi_\beta, 2\pi/\omega] \cup [0, \phi_\alpha].$$

If $\sigma = 0$ and $f(t) = \cos(\omega t)$ then $\phi_\alpha = \pi/2\omega$ and $\phi_\beta = 3\pi/2\omega$; moreover if $\sigma > 1$ then I is the empty set.

When combined with chatter, the sticking region plays a major role in the dynamics of the impact oscillator. This is because it has a large domain of attraction $\mathscr{F}$ comprising those trajectories which come to rest following a chattering sequence. Part of the purpose of this paper is to construct the set $\mathscr{F}$. This set occupies a significant proportion of the domain of definition of the map P and consequently is likely to be robust to changes in the model given in (1). It is highly significant that for all $\phi \in I$,

$$P(\phi, 0) = P(\phi_\alpha, 0),$$

and hence P is not invertible over the set I.

By far the most significant aspect of P, realized by Shaw & Holmes (1983) and developed by Whiston (1992), D. Chillingworth (unpublished notes), Nordmark (1991) and Foale & Bishop (1992) is that it is discontinuous on a one dimensional set S^1 in the phase space and, more importantly, that it introduces considerable stretching onto the phase space in a neighbourhood of S^1. We shall review this behaviour in the next section. Away from the set S^1, the map P is smooth and it behaves very like any other nonlinear map of two variables, with fixed points that undergo various standard forms of bifurcation. However, the discontinuity and stretching result in the many new forms of behaviour remarked upon in the literature.

A very good illustration of this richness of the behaviour of impact oscillators and the role played by chatter is provided by studying the domain of attraction of the fixed points of P for certain parameter values. If, for example, $\omega = 2.6$, $\sigma = 0$ and $r = 0.8$ then P has both the fixed point $A \equiv (\frac{1}{2}\omega\phi/\pi, v) \equiv (0.482\,14, 0.505\,44)$ and the period-6 orbit B, where

$$B = \{(\tfrac{1}{2}\omega\phi/\pi, v)\} \equiv \left\{ \begin{matrix} (0.285, 0.554), (0.486, 0.907), (0.632, 0.443), \\ (0.272, 0.563), (0.481, 0.934), (0.635, 0.472). \end{matrix} \right\}$$

Both A and B correspond to periodic motions of the impact oscillator of periods $2\pi/\omega$ and $12\pi/\omega$ respectively. A large number of numerical simulations indicate strongly that these are the only two forms of stable asymptotic motion of the impact oscillator for these ranges of the parameter values. In figure 4 we plot the domains of attraction for these two orbits for a range of initial conditions, $[\phi, v] \in [0, 2\pi/\omega] \times [0, 4]$. Also indicated on this figure are the orbits A, B and the sticking region I.

The figure has a beautiful and complex form demonstrating the interesting fact that even if a system has only two periodic asymptotic states, the asymptotic motion of the particle can be very sensitive to its initial condition. The sensitivity is caused by the large and intertwined domains of attraction of A and B resulting from the stretching and discontinuity of the phase space introduced by P. The complexity of the domain of attraction can be understood by examining the structure of the set S^1, its preiterates and the intersection of these sets with the domain of attraction, $\mathscr{F}$ of the sticking region I. We can see part of this structure by observing from figure 4 that

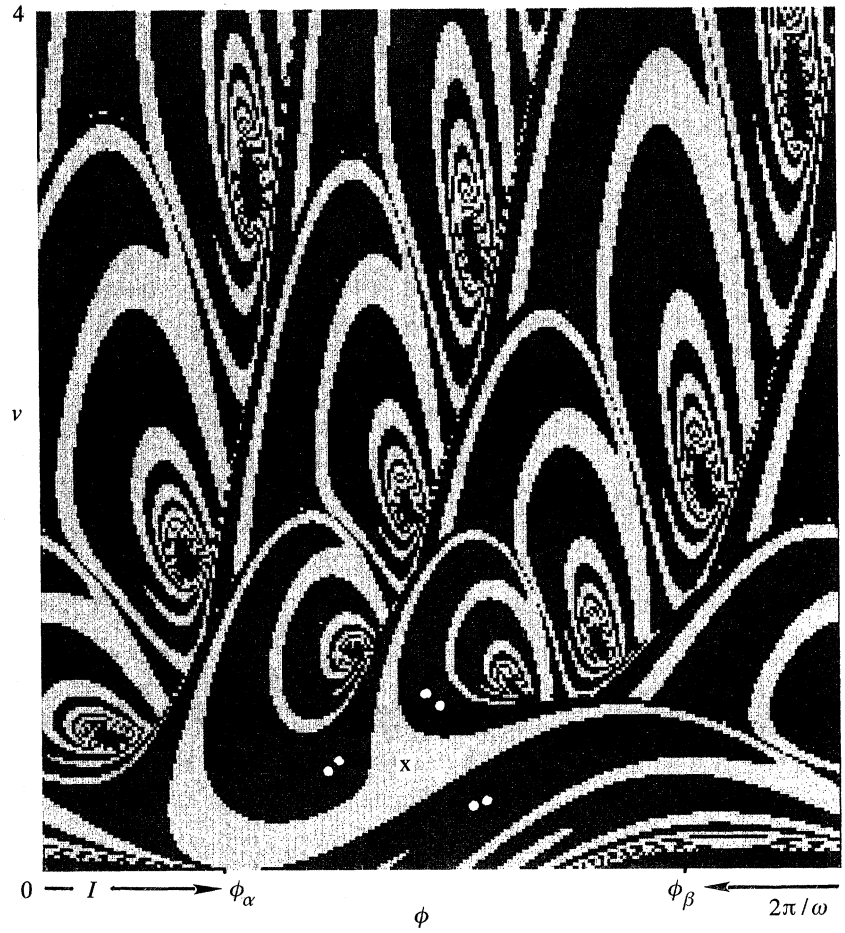

Figure 4. The domains of attraction for the $(1,1)$ (light shade) and the $(6,6)$ (dark shade) periodic orbits when $\omega = 2.6$ and $\sigma = 0$. The $(1,1)$ orbit is indicated by a cross and the $(6,6)$ orbit by six circles.

there is a neighbourhood $\mathscr{D}$ of I all of which is attracted to B as is each of its pre-images under P. This neighbourhood is indeed a subset of $\mathscr{F}$ which is composed of $\mathscr{D}$ and its pre-images. Moreover, the domains of attraction of A and B close to the boundary, $\mathscr{C}$, of $\mathscr{D}$ have a very fine structure with close by points being attracted to either attractor. The images and pre-images of both $\mathscr{D}$ and its boundary form large loops in the phase space and these can also be seen in figure 4. A major purpose of this paper is an explanation of this structure in detail. Similar structures are observed for the domains of attraction of different orbits for other parameter values and are due to the same underlying mechanism.

The outline of the rest of this paper is as follows. In §2 we review some of the theory of the stretching behaviour of the map P and of the discontinuity set S^1. In §3 we demonstrate the existence of both chattering and incomplete chattering behaviour, and construct an invariant set $\mathscr{D}$ for P such that all orbits starting in $\mathscr{D}$ lead to chattering motion followed by sticking. By examining the behaviour of P close to the boundary of $\mathscr{D}$ we show that it can be simplified to a one dimensional map with a consequent simplification in the analysis of the dynamics. In §4 we compute

the pre-images of $\mathscr{D}$ to calculate the domain of attraction $\mathscr{F}$ of the sticking region, demonstrating the existence of loops in the boundary of this set. Using this information we deduce the form of the domains of attraction for the attractors of P. In §5 we show how chatter can form part of a periodic motion and show how this is related to certain types of chaotic behaviour. Finally, in §6 we draw some conclusions from this work.

2. The stretching associated with P

The map P which was defined in §1 has many interesting properties and some of these are reviewed in Whiston (1992), Nordmark (1991) and Foale & Bishop (1992). Of most interest to us here are the two facts that it can have periodic points $\boldsymbol{x}$ such that $P^m(\boldsymbol{x}) = \boldsymbol{x}$ for some integer m, and that it is discontinuous on a set S^1, and smooth away from S^1.

The periodic points also correspond to (subharmonic) trajectories which repeat after a time $2\pi n/\omega$ and we label them by the indices (m, n). As parameters such as ω and σ are varied, the periodic points display similar behaviour to the periodic points of smooth maps (including period-doubling and saddle-node bifurcations) until one of the iterates of $\boldsymbol{x}$ intersects the line S^1.

For the remainder of this section we discuss some of the basic properties of S^1 and the behaviour of P in a neighbourhood of S^1. Although it is rather technical we include it because of the insight it gives into the general dynamics of the particle. (This discussion will review the results presented in Nordmark (1991), Whiston (1992) and Budd & Dux (1994) and will necessarily be very incomplete.)

We suppose that we have three impacts at points A, B, C which have similar phases and velocities. We suppose further that $P(A) = (\phi_1, v_1)$ where v_1 is close to zero and that $P(B) = (\phi_2, 0)$ where ϕ_1 is close to ϕ_2, but that the trajectory with initial condition C has a maximum with phase ϕ_m close to ϕ_2 so that the next impact occurs at a rather different phase ϕ_3, so that $P(C) = (\phi_3, v_3)$.

The map P is then discontinuous at the point B. In a sense this discontinuity is artificial in that $P^2(A) \approx P^2(B) \approx P(C)$ and, indeed, the trajectories starting from A, B and C are similar. However, the discontinuity introduces considerable sensitivity to the initial conditions (or stretching in the phase space) and this plays a major role in the overall behaviour of the impact oscillator.

(a) *Local behaviour of P close to S*

To make this behaviour precise we introduce the following notation first used by Whiston (1992) for the discontinuity set and its iterates and pre-iterates:

$$S^1 = \{(\phi, v) : P(\phi, v) = (\phi_2, 0)\}, \quad S^n = \{(\phi, v) : P^n(\phi, v) = (\phi_2, 0)\}$$

and

$$W^n = \{(\phi, v) : (\phi, v) = P^n(\phi_2, 0)\},$$

so that

$$W^1 = P^2(S^1).$$

The sets W^n and S^n are dual; indeed by exploiting the time reversal symmetry of the impact oscillator we have

$$S^1 = \{(\phi, v) : [(2\pi/\omega) - \phi, rv] \in W^1\}.$$

Close to S^1, the map P causes considerable stretching of the phase space and the effect of this is illustrated in figure 5 and discussed in detail in Whiston (1992),

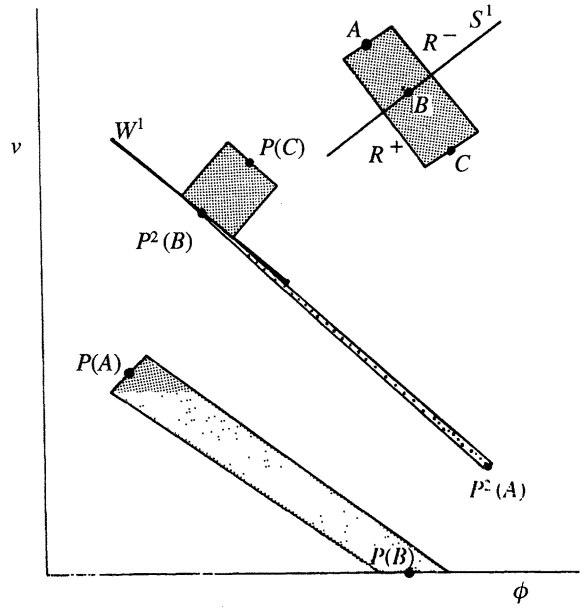

Figure 5. The stretching of the phase space produced by the map P close to the discontinuity set S^1.

Nordmark (1991), Foale & Bishop (1992) and Budd & Dux (1994). In this figure we consider a rectangle $R = R^+ \cup R^-$ of initial data which intersects the set S^1 and is bounded by line segments through the points A, $B \in S$ and C which were considered earlier. Thus the subsets R^+ and R^- lie on either side of S^1 and R^- includes part of S^1. The subset R^- comprises the initial data which is mapped to low velocity impacts and the effect of these is to stretch R^- to a set intersecting the set $v = 0$ which is parallel to the vector $\begin{pmatrix} -1 \\ -N \end{pmatrix}$, where $N \equiv f(\phi_2) - \sigma$ is the local acceleration of the particle at the point $P(B)$. Indeed the stretching factor approaches infinity as we approach B. On the further action of the map P, the set $P(R^-)$ is contracted in the direction $\begin{pmatrix} r \\ -N \end{pmatrix}$ and is mapped to a set which is locally tangent to W^1, intersecting W^1 in a set which includes the point $P^2(B)$. The map from R^- to $P^2(R^-)$ introduces a pronounced stretching between two data points connected by a line orthogonal to S^1, but not between two points connected by a line parallel to S^1.

In contrast, the subset R^+, comprises those points which must miss an impact at the point $P(B)$. This set is not stretched at all by P, and the set $P(R^+)$ approaches W^1 transversally, with $P(R^+)$ and $P^2(R^-)$ lying on either side of W^1. (We note that the stretching behaviour applies to much more general systems than the (linear) impact oscillators discussed here.)

(*b*) *The global behaviour of the sets S^n and W^n*

It was first recognized in Whiston (1992) that the global dynamics of the map P is largely governed by the global structure of the sets S^n and W^n. To gain some insight into this structure we display, in figure 6, the set

$$S^1 \cup S^2 \cup S^3 \cup W^1 \cup W^2 \cup W^3$$

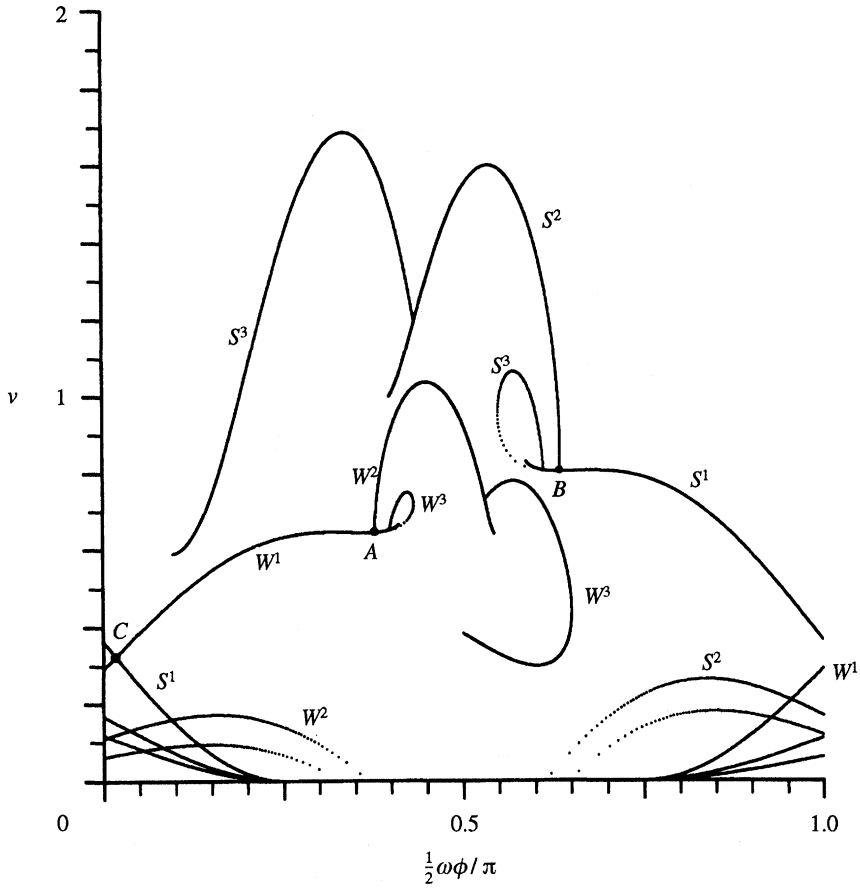

Figure 6. The set $S^1 \cup S^2 \cup S^3 \cup W^1 \cup W^2 \cup W^3$.

when $r = 0.8$, $\sigma = 0$ and $\omega = 2.6$. (It is interesting to compare this figure with the domain of attraction for the same parameter values presented in figure 4.) Some of the structure of these sets, particularly as σ is varied, can be complex and Whiston (1992) and D. Chillingworth (unpublished notes) devote much space to describing it. However, the general outline of figure 6 can be described fairly simply. To do this we first consider the set W^1 and its iterates W^n. The nature of the sets S^n is essentially equivalent to that of W^n and may be deduced in a similar manner by reversing the direction of time in the impact oscillator and replacing r by $1/r$.

The sets W^n are given by $W^n = P^n(\phi, 0)$ for $0 < \phi < 2\pi/\omega$. If $\phi \in I$ then the particle remains stuck to the obstacle and we may consistently define $W^n = (\phi, 0)$ for all values of n. At the point $\phi = \phi_\alpha$ the particle becomes unstuck and the point $P^n(\phi_\alpha, 0)$ is than an end-point for W^n. Equivalently the point $P^{-n}(\phi_\beta, 0)$ is an end point for S^n. As ϕ increases away from ϕ_α, the curves W^n describe smooth loci until (for example) W^1 intersects S^1 at the point C when (say) $\phi = \phi_S$. At this point we apply the results of the last section to calculate the locus of W^2. Indeed W^n divides into two disconnected curves for $\phi < \phi_S$ and $\phi \geqslant \phi_S$ one of which (given by $\phi < \phi_S$) approaches (but does not intersect) W^1 at the point A indicated on figure 6 and the other intersects the line $\{v = 0\}$ when $\phi = \phi_S$. Similarly, W^3 intersects W^1 tangentially at A when $\phi \geqslant \phi_S$. By reversing time a very similar behaviour is observed when S^1

intersects W^1 in that S^2 is divided into two subsets, one of which approaches S^1 transversally at the indicated point B and the other intersects the line $\{v = 0\}$. Moreover, the set S^3 intersects S^1 tangentially at B.

As ϕ increases to ϕ_β the sets W^n tend toward the point $(\phi_\beta, 0)$ and have an approximately parabolic form close to this point. Similarly the sets S^n tend toward parabolae passing through the point $(\phi_\alpha, 0)$. We describe this behaviour in detail in §3.

The simple observations account for much of the structure of figure 6 and this basic structure is, in general, preserved for other values of ω, σ and also when damping between impacts is included in the model. In the following sections we see how, by including chatter into the dynamics, we can predict much of the global behaviour of P (and the forms of the domains of attraction) from these observations of the forms of W^n and S^n.

3. Chatter and the invariant chattering region

We now turn our attention to the main theme of this paper: namely the existence of chattering orbits and the role played by chatter on the dynamics of the impact oscillator. Loosely speaking, a chattering motion is one that involves an infinite number of low velocity impacts with the obstacle before the particle comes to rest against it with some phase ϕ_∞ in the sticking region. Similar phenomena have been observed in the (chaotic) motion of billiard balls (Katok & Strelcyn 1980) where they are referred to as 'dead end orbits'.

To be precise, we define an orbit to include chatter if it contains a sequence (ϕ_n, v_n) such that

$$(\phi_n, v_n) \to (\phi_\infty, 0) \quad \text{as} \quad n \to \infty,$$

where $\phi_\infty \in I$. We can also have various forms of incomplete chatter in which there are a large number of low velocity impacts in a short time interval, but at some critical value of N, $\phi_N > \phi_\alpha$ and, as the acceleration of the particle is now away from the obstacle, the phase of the next impact ϕ_{N+1} is then rather different from ϕ_N.

Any motion which includes chatter must include the point $(\phi_\alpha, 0)$. Hence if chatter repeats then the orbit is necessarily periodic. However, the motion can still be very complex, especially if the image of the point $(\phi_\alpha, 0)$ is close to a saddle-point of the map P.

In this section we show that chattering orbits define a basin of attraction $\mathscr{D}$ for the sticking region I, formed by the pre-images of the orbits which include chatter. Moreover, $\mathscr{D}$ is bounded by a set $\mathscr{C}$ which is an accumulation set for the sets S^n as $n \to \infty$.

For simplicity, our discussion will be mainly concerned with the forcing function $f(t) = \cos(\omega t)$. However, many of the conclusions apply as well to more general differentiable, periodic forcing functions $f(t)$ such that $f(t) - \sigma$ changes sign at the two points ϕ_α and ϕ_β.

(a) *The dynamics of a chattering motion*

To demonstrate the existence of a chattering motion when $f(t) = \cos(\omega t)$ we presume that the particle has an initially low velocity for some value of $\phi_0 \in I$, where ϕ is not too close to the end points of I. In this case we have a positive acceleration toward the obstacle and we may presume that the time to the next impact is small. If we take $\mathrm{d}x/\mathrm{d}t = -rv_0 \ll 1$ at phase ϕ_0 then

$$\mathrm{d}^2x/\mathrm{d}t^2 = \cos(\omega\phi_0) - \sigma, \quad \mathrm{d}^3x/\mathrm{d}t^3 = -\omega\sin(\omega\phi_0) + rv_0, \quad \text{etc.}$$

Thus, if $\Lambda \equiv \phi - \phi_0$, we may express the local behaviour of the particle in terms of a Taylor series so that

$$x = \sigma - rv_0 \Lambda + \tfrac{1}{2}(\cos(\omega\phi_0) - \sigma)\Lambda^2 - \tfrac{1}{6}(\omega \sin(\omega\phi_0) - rv_0)\Lambda^3 + O(\Lambda^4), \tag{3}$$

$$\dot{x} = -rv_0 + (\cos(\omega\phi_0) - \sigma)\Lambda - \tfrac{1}{2}(\omega \sin(\omega\phi_0) - rv_0)\Lambda^2 + O(\Lambda^3). \tag{4}$$

The time to the next impact is given by the first value of Λ for which $x(\Lambda) = \sigma$. If v_0 is small then Λ is also small and to leading order in v_0 the value of Λ is given by

$$\Lambda = 2rv_0/[\cos(\omega\phi_0) - \sigma]. \tag{5}$$

This approximation is reasonable provided that

$$(\omega \sin(\omega\phi_0) + rv_0)\Lambda \ll (\cos(\omega\phi_0) - \sigma),$$

so that

$$v_0 \ll (\cos(\omega\phi_0) - \sigma)^2/(\omega \sin(\omega\phi_0) + rv_0). \tag{6}$$

We assume this to be the case for the present and return to it in the next section.

It follows from (5) that the next impact occurs at the phase ϕ_1, where

$$\phi_1 = \phi_0 + 2rv_0/[\cos(\omega\phi_0) - \sigma]. \tag{7}$$

Combining (4) and (5) gives the velocity at the next impact as

$$v_1 = rv_0. \tag{8}$$

Thus, provided that condition (6) is met, (7) and (8) give a simplification of the impact map P for small velocities v_0 and for $\phi \in I$. A similar simplification can be made for a wide class of forcing functions $f(t)$.

For any value of $\phi_\infty \in I$ this map has a fixed point given by $(\phi, v) = (\phi_\infty, 0)$ corresponding to a chattering trajectory which has come to rest at this point. If ϕ_n is close to ϕ_∞ and v_n close to 0 then we can linearize the map about this point to give

$$\phi_{n+1} \approx \phi_n + 2rv_n/[\cos(\omega\phi_\infty) - \sigma], \quad v_{n+1} \approx rv_n. \tag{9}$$

Thus the local behaviour of the iterates of P is given by

$$v_n \approx r^n v_0, \quad \phi_n \approx \phi^\infty - 2r^{n+1}v_0/[(1-r)(\cos(\omega\phi_\infty) - \sigma)]; \tag{10}$$

an infinite number of collisions of ever decreasing velocity occurring in a finite time.

The formulae (9) and (10) give the approximate dynamics of P close to the fixed point and it is evident from this that the points (ϕ_n, v_n) lie on the straight line passing through $(\phi_\infty, 0)$ given by

$$v_n = \tfrac{1}{2}(1-r)(\cos(\omega\phi_\infty) - \sigma)(\phi_\infty - \phi_n)/r. \tag{11}$$

The gradient of these lines is $-\tfrac{1}{2}(1-r)(\cos(\omega\phi_\infty) - \sigma)/r$ which takes its maximum value when $\phi_\infty = 0$ and its minimum of zero when $\phi_\infty = \phi_\alpha$ or $\phi_\infty = \phi_\beta$. When studying the trajectory of a chattering motion we should, in general, expect to see a set of points which approaches the line $v = 0$ along such a straight line. In figure 7 we illustrate such a trajectory for which the first few iterations do not have a clear structure but eventually do become asymptotic to a straight line.

(*b*) *The invariant region* $\mathscr{D}$

The analysis of chatter presented above gives the final behaviour of a chattering trajectory but does not clearly indicate what initial conditions (other than 'sufficiently small v_0') inevitably lead to such a trajectory. We now address this

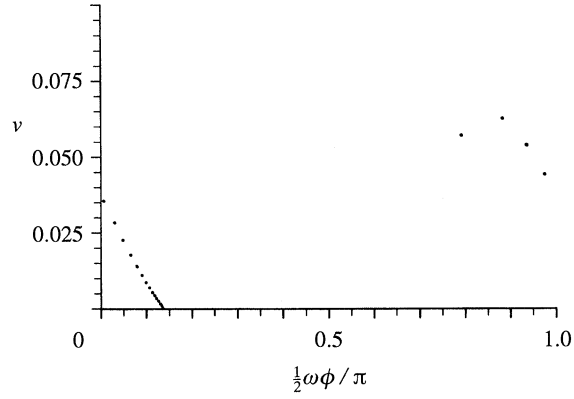

Figure 7. The iterates of P for an orbit which includes chatter.

question by calculating a neighbourhood $\mathscr{D}$ of I which is mapped into itself by P and has the property that any trajectory starting in it inevitably experiences chatter before coming to rest.

Surprisingly, we can calculate this region by examining the behaviour of the map P close to the end points $(\phi_\alpha, 0)$ and $(\phi_\beta, 0)$ of I. We do this by considering the action of P on a series of parabolae T_λ parametrized by λ passing through the point $(\phi_\alpha, 0)$. The structure of the map P close to ϕ_α is then completely characterized by the effect it has on each such parabola and we express this in the following lemma.

Lemma 1. *Let* $T_\lambda = \{(\phi, v): v = \omega\lambda(\phi_\alpha - \phi)^2, \phi \leqslant \phi_\alpha\}$; *then if* $(\phi - \phi_\alpha)$ *is sufficiently small,*

$$P(T_\lambda) = T_\mu,$$

where $\mu = f(\lambda)$ *and*

$$f(\lambda) = (-r\lambda + \sin(\omega\phi_\alpha)\, T - \tfrac{1}{2}\sin(\omega\phi_\alpha)\, T^2)/(1-T)^2,$$

where

$$T = \tfrac{3}{2} - \tfrac{1}{2}\sqrt{[9 - 24r\lambda/\sin(\omega\phi_\alpha)]}.$$

In other words, a parabolic set of initial conditions is mapped to another such set. (This result remains true for any sufficiently smooth forcing function.)

Proof. We again use the Taylor series decomposition

$$x = \sigma - rv_0 \Lambda + \tfrac{1}{2}(\cos(\omega\phi_0) - \sigma)\, \Lambda^2 - \tfrac{1}{6}(\omega \sin(\omega\phi_0) - rv_0)\, \Lambda^3 + O(\Lambda^4).$$

We now presume that $(\phi_0, v_0) \in T_\lambda$ and that $\phi_0 = \phi_\alpha - \varepsilon$, where $\cos(\omega\phi_\alpha) - \sigma = 0$ and ε is small. Then

$$\cos(\omega\phi_0) - \sigma = \cos(\omega(\phi_\alpha - \varepsilon)) - \sigma = \omega\varepsilon \sin(\omega\phi_\alpha) + O(\varepsilon^2),$$
$$\omega \sin(\omega\phi_0) = \omega \sin(\omega\phi_\alpha) + O(\varepsilon).$$

Now, by definition, $v_0 = \omega\lambda\varepsilon^2$. Thus

$$x = \sigma - r\varepsilon^2\omega\lambda\Lambda + \tfrac{1}{2}\varepsilon\omega \sin(\omega\phi_\alpha)\, \Lambda^2 - \tfrac{1}{6}(\omega \sin(\omega\phi_\alpha) - r\omega\lambda\varepsilon^2)\, \Lambda^3 + O(\varepsilon^2\Lambda^2) + O(\varepsilon\Lambda^3) + O(\Lambda^4).$$

To solve this to find Λ such that $x = \sigma$, we put $\Lambda = \varepsilon T$, where T is of order 1, giving

$$0 = -r\omega\lambda + \tfrac{1}{2}\omega \sin(\omega\phi_\alpha)\, T - \tfrac{1}{6}\omega \sin(\omega\phi_\alpha)\, T^2 + O(\varepsilon^2).$$

If we then ignore terms of $O(\varepsilon^2)$ we find that T satisfies the quadratic equation

$$\tfrac{1}{6}\sin(\omega\phi_\alpha)\,T^2-\tfrac{1}{2}\sin(\omega\phi_\alpha)\,T+r\lambda=0.$$

The corresponding equation for $\dot{x}$ is

$$\dot{x}=-r\varepsilon^2\omega\lambda+\varepsilon\omega\sin(\omega\phi_\alpha)\,\Lambda-\tfrac{1}{2}\omega\sin(\omega\phi_\alpha)\,\Lambda^2+O(\varepsilon^2\Lambda).$$

Substituting $\Lambda=\varepsilon T$ gives the velocity v_1 at the next impact as

$$v_1=\varepsilon^2\omega[-r\lambda+\sin(\omega\phi_\alpha)\,T-\tfrac{1}{2}\sin(\omega\phi_\alpha)\,T^2]. \tag{12}$$

Now, the phase of the next impact is $\phi_1\equiv\phi_0+\Lambda$, so that

$$\begin{aligned}\phi_1&=\phi_\alpha-\varepsilon+T\varepsilon\\&=\phi_\alpha-\varepsilon(1-T),\end{aligned}$$

or

$$\phi_\alpha-\phi_1=\varepsilon(1-T).$$

Combining this with (12) gives

$$v_1=\omega\mu(\phi_\alpha-\phi_1)^2,\ (\phi_1,v_1)\in T_\mu,$$

where $$\mu=[-r\lambda+\sin(\omega\phi_\alpha)\,T-\tfrac{1}{2}\sin(\omega\phi_\alpha)\,T^2]/[1-T]^2.$$

Now, T satisfies the quadratic equation

$$T^2-3T+[6r\lambda/\sin(\omega\phi_\alpha)]=0.$$

So

$$T=\tfrac{3}{2}\pm\tfrac{1}{2}\sqrt{[9-24r\lambda/\sin(\omega\phi_\alpha)]}.$$

We take the negative root in this expression to ensure that T gives the phase of the first impact after ϕ_0. Combining our expressions gives the formula for f in the Lemma. □

The significance of this result is that close to ϕ_α we can simplify the map P to a one dimensional map from the set T_λ to the set T_μ characterized by the single function f.

After some manipulation, we can show that f has the following properties:

$$f(0)=0;\quad \mathrm{d}f/\mathrm{d}\lambda\,(0)=r<1;\quad \mathrm{d}^2f/\mathrm{d}\lambda^2\,(\lambda)>0\quad\text{for all}\quad\lambda<\sin(\omega\phi_\alpha)/3r;$$
$$\mathrm{d}^2f/\mathrm{d}\lambda^2\,(0)=20\,r^2/[3\sin(\omega\phi_\alpha)];\quad f(\lambda)\to\infty,\,T\to1\quad\text{as}\quad\lambda\to\sin(\omega\phi_\alpha)/3r.$$

The general form of $f(\lambda)$ is illustrated in figure 8, together with the line $g(\lambda)=\lambda$, and the intersection of these demonstrates the existence of a fixed point of f.

Combining these simple results gives the following important lemma.

Lemma 2. (i) *The function $f(\lambda)$ has a unique non-zero fixed point λ_∞ where $\frac{1}{3}\sin(\omega\phi_\alpha)/r>\lambda_\infty>0$ such that $f(\lambda_\infty)=\lambda_\infty$ and a further fixed point $\lambda=0$.*

(ii) *If $\sin(\omega\phi_\alpha)/3r>\lambda>\lambda_\infty$ then $f(\lambda)>\lambda$.*

(iii) *If $\lambda<\lambda_\infty$ then $f(\lambda)<\lambda$ and $f^n(\lambda)\to0$ as $n\to\infty$.*

By using the local information on f close to the origin we have that for small λ

$$f(\lambda)\approx r\lambda+[10r^2\lambda^2/3\sin(\omega\phi_\infty)].$$

If r is close to one we may use this expression to compute λ_∞; indeed

$$\lambda_\infty\approx\frac{3}{10}\frac{(1-r)}{r^2}\sin(\omega\phi_\infty).$$

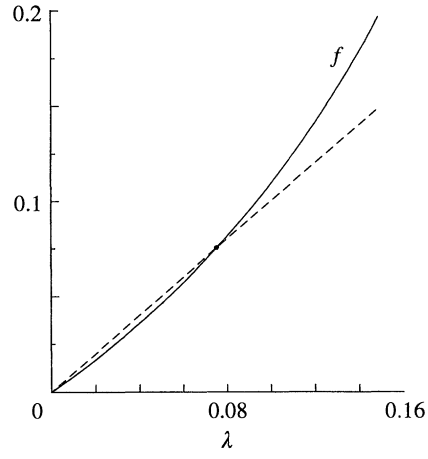

Figure 8. The function $f(\lambda)$.

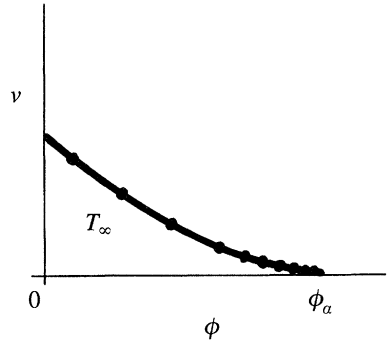

Figure 9. The parabola T_∞ and the locus of a chattering orbit for which $\phi_\infty = \phi_\alpha$.

Lemma 2 is a most important result because if we are sufficiently close to the point $(\phi_\alpha, 0)$, so that the approximations we have made are negligible, we can deduce from it the existence of a curve which is invariant under the action of P.

Corollary. *If ϕ is close to ϕ_α then the curve*

$$T_\infty \equiv T_{\lambda_\infty} = \{(\phi, v) : v = \omega\lambda_\infty(\phi_\alpha - \phi)^2\}$$

is invariant under the action of P.

Any chattering orbit for which $\phi_\infty \equiv \phi_\alpha$ must ultimately lie on the parabola T_∞ and we illustrate this in figure 9. Indeed, a point on T_∞ will move monotonically to the right, converging to the point $(\phi_\alpha, 0)$.

In fact, the arc of the parabola T_∞ with end-point $(\phi_\alpha, 0)$ is a limit for an invariant curve of the map P as $\phi \to \phi_\alpha$. Further away from ϕ_α the terms of $O(\varepsilon^2)$, which we have neglected in the expressions for x and v, become important and while P continues to have an invariant curve, this set departs from being a simple parabola. (We note that this is not a rigorous proof of the existence of such a curve which would need more careful arguments than those given here such as a fixed point construction in an appropriate function space. However, the arguments here do demonstrate how such a curve can be constructed.) To compute this invariant curve we take a small arc of

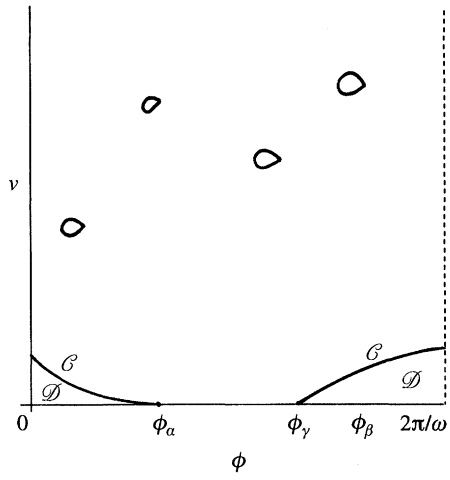

Figure 10. The pre-iterates of the parabola T_∞, illustrating the set $\mathscr{C}$ and the invariant region $\mathscr{D}$.

the parabola T_∞ with $(\phi_\alpha, 0)$ as an end-point and iterate this set backwards under the action of P^{-1}. This defines a complex set of curves which are not all connected and some of these are illustrated in figure 10.

From this figure we identify an arc, also with end-point $(\phi_\alpha, 0)$, which further intersects the line $v = 0$ at the point $(\phi_\gamma, 0)$ where

$$\phi_\gamma < \phi_\beta < 2\pi/\omega.$$

The image of $(\phi_\gamma, 0)$ under P is the first point where the backward iterates of the arc of T_∞ intersects the set W^1. We denote this curve by $\mathscr{C}$, and the region enclosed between itself and the line $v = 0$ by $\mathscr{D}$. We make the assumption at this point that the map P has no fixed points lying either on $\mathscr{C}$ or in $\mathscr{D}$ and the closely related assumption that the set S^1 does not intersect $\mathscr{C}$. It follows from these assumptions that P is smooth and invertible within $\mathscr{D}$. Now, as both $\mathscr{C}$ and the line I are invariant under the action of P, it then follows that $\mathscr{D}$ will be an invariant set (under the forward action of P) and, by the assumption on the fixed point of P, any trajectory with an initial point in $\mathscr{D}$ must inevitably lead to chatter.

We can show further that, under these assumptions, the curve $\mathscr{C}$ is an accumulation set for the curves S^n. We establish this in the following lemma.

Lemma 3. (i) *If ϕ is close to ϕ_α, then S^1 has a component which coincides with the parabola $T_{\frac{3}{8}\sin(\omega\phi_\alpha)/r}$.*

(ii) *As $n \to \infty$, S^n has a component which coincides with the set of parabolae T_{λ_n} where λ_n is monotonically decreasing, $f(\lambda_n) = \lambda_{n-1}$, $\lambda_1 = \frac{3}{8}\sin(\omega\phi_\alpha)/r$ and $\lambda_n \to \lambda_\infty$ as $n \to \infty$.*

Proof. The discontinuity set S^1 is the set of points (ϕ_0, v_0) for which

$$P(\phi_0, v_0) = (\phi_1, 0).$$

If we assume that $\phi_0 \approx \phi_\alpha$ and we set $v_1 = 0$ in (12), then T and λ must satisfy the relation

$$-r\lambda + \sin(\omega\phi_\alpha)\, T - \tfrac{1}{2}T^2 \sin(\omega\phi_\alpha) = 0,$$

so that

$$T^2 - 2T + [2r\lambda/\sin(\omega\phi_\alpha)] = 0.$$

But T must also satisfy the quadratic equation

$$T^2-3T+[6r\lambda/\sin(\omega\phi_\alpha)]=0.$$

Combining these two equations gives

$$T=\tfrac{3}{2} \quad \text{and} \quad \lambda=\tfrac{3}{8}\sin(\omega\phi_\alpha)/r.$$

Hence to leading order, S^1 has a component given by the parabola T_{λ_1} where

$$\lambda_1=\tfrac{3}{8}\sin(\omega\phi_\alpha)/r>\tfrac{1}{3}\sin(\omega\phi_\alpha)/r>\lambda_\infty.$$

Proceeding as before, S^n has a component given by T_{λ_n} where

$$\lambda_n=f^{-1}(\lambda_{n-1})$$

and by the previous calculation, $\lambda_n>\lambda_\infty, \lambda_n<\lambda_{n-1}$ and $\lambda_n\to\lambda_\infty$ as $n\to\infty$. □

The above lemma gives a precise description of the sets S^n close to the point $(\phi_\alpha, 0)$ which is in accord with the observations recorded in figure 6.

We conclude that under the assumptions about the fixed points of P, the curve $\mathscr{C}$ and the line $v=0$ bound a region $\mathscr{D}$ with the following properties.

Theorem 1. (i) *The region $\mathscr{D}$ is an invariant region for P and any orbit starting within it experiences chatter before sticking.*

(ii) *The boundary of $\mathscr{D}$ is an invariant curve $\mathscr{C}$.*

(iii) *$\mathscr{C}$ is an accumulation set for the curves S^n as $n\to\infty$.*

We can say a little more about the shape of $\mathscr{D}$ by considering the points of intersection between $\mathscr{C}$ and the sets W^n considered in the last section. These sets have a structure which, in a neighbourhood of the point $(\phi_\beta, 0)$ is very similar to that of S^n and is given by the following result.

Lemma 4. *Let $U_\lambda=\{(v,\phi): v=\omega\lambda(\phi-\phi_\beta)^2,\ \phi\geqslant\phi_\beta\}$.*

(i) *If ϕ is sufficiently close to ϕ_β then*

$$P(U_\lambda)=U_\mu,$$

where $$\mu=g(\lambda)=[-r\lambda+\sin(\omega\phi_\alpha)\,T+\tfrac{1}{2}\sin(\omega\phi_\alpha)\,T^2]/(1+T)^2$$

and T satisfies the quadratic equation

$$T^2+3T-[6r\lambda/\sin(\omega\phi_\alpha)]=0.$$

(ii) *In a neighbourhood of $(\phi_\beta, 0)$*

$$W^1=U_{\lambda_1} \quad \lambda_1=\tfrac{3}{8}\sin(\omega\phi_\alpha)$$

and $$W^n(\phi,v)=U_{\lambda n}, \quad \textit{where} \quad \lambda_n=g(\lambda_{n-1}).$$

(iii) *As $n\to\infty$, $W^n\to\{v=0\}$.*

Proof. The proof of this result is similar to that for S^1 and follows by taking a Taylor series expansion close to $(\phi_\beta, 0)$. For simplicity we shall omit it. □

The map $g(\lambda)$ is very similar to $f(\lambda)$; however it has the significant difference that

$$\mathrm{d}g/\mathrm{d}\lambda\,(0)=r, \quad \mathrm{d}^2g/\mathrm{d}\lambda^2\,(\lambda)<0, \forall\,\lambda>0.$$

Thus it has no fixed points other than $\lambda=0$ and hence $\lambda_n\to 0$ so that

$$W^n\to\{v=0\} \quad \text{as} \quad n\to\infty.$$

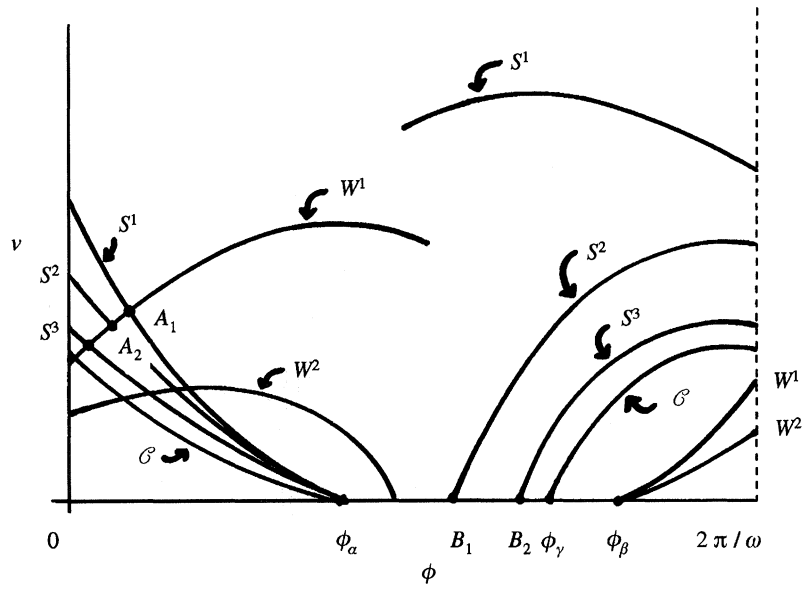

Figure 11. The form taken by the sets S^n and W^n in the neighbourhood of the set $\mathscr{C}$.

The resulting form of $\mathscr{C}$, and of the sets S^n and W^n in a neighbourhood of I is illustrated in figure 11.

To complete our description of the invariant set $\mathscr{D}$ we note from figure 11 that the sets S^1 and W^1 intersect at a point A_1 which is close to $\mathscr{C}$. Similarly, W^1 intersects the sets S^n at a sequence of such points A_n accumulating at the point A_∞ where W^1 intersects $\mathscr{C}$.

We define B_n to be the pre-image of A_n so that $B_n = P^{-1}(A_n)$ and

$$B_n \in S^{n+1} \cap \{v = 0\}.$$

It follows that $B_n \to B_\infty$, where $B_\infty = (\phi_\gamma, 0)$ is the point where $\mathscr{C}$ intersects the line $v = 0$, so that if $B_n = (\phi_n, 0)$ then $\phi_n \to \phi_\gamma < \phi_\beta$ as $n \to \infty$. We can also deduce the structure of $\mathscr{C}$ close to the point B_∞, by studying the pre-image of the set S^n close to its intersection with W^1. It follows from the discussion in §2(*b*) that this is a portion of the set S^{n+1} passing through B_n, and that close to B_n this set approximates a straight line of gradient $1/[r(\sigma - \cos(\phi_n))]$. Taking the limit as $n \to \infty$ we deduce that close to B_∞ the curve $\mathscr{C}$ approximates a straight line of gradient $1/[r(\sigma - \cos(\phi_\gamma))]$.

(*c*) *Incomplete chatter*

We conclude this section by looking at those trajectories which have a large number of low velocity impacts but do not ultimately stick to the obstacle. Such a trajectory must include a point which lies close to the curve $\mathscr{C}$ but not inside the region $\mathscr{D}$. The iterates of this point will then initially lie close to $\mathscr{C}$ and will have low velocity impacts, but will eventually leave a neighbourhood of $\mathscr{C}$ after a finite number of iterations. The closer the initial point is to $\mathscr{C}$, the more low impacts will be included in the motion. We can estimate the curve dividing those low velocity impacts that lead to further such impacts at a nearby time from those that lead to high velocity impacts at a rather later time, by the set S^1. Indeed, those points lying to the 'left' of S^1 are mapped to a neighbourhood of $\mathscr{C}$, whereas those lying to the

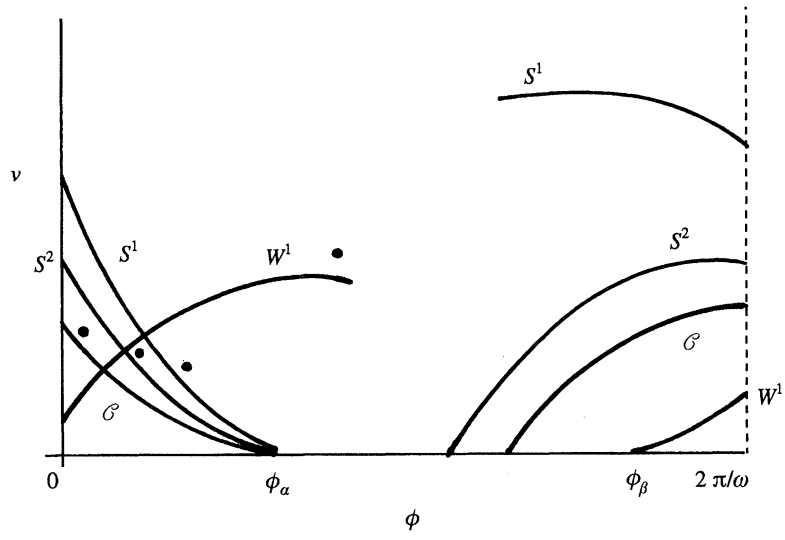

Figure 12. The iterates of a trajectory which includes a sequence of incomplete chatter.

'right' are mapped to that part of W^1 which is close to $P(\phi_\alpha, 0)$. We illustrate this in figure 12 by plotting the iterates of P corresponding to a trajectory which includes a sequence of impacts with incomplete chatter.

4. Domains of attraction

For various values of ω and σ, the map P has distinct periodic attractors (for example $\omega = 2.6$, $\sigma = 0$) and, as we saw in the introduction, the domains of attraction of each such attractor can have a complex form. Much of this complexity can, however, be understood by examining the images and pre-images of the set $\mathscr{D}$ constructed in the last section. This follows partly from the following simple result.

Lemma 5. *All points in $\mathscr{D}$ and its pre-images have the same asymptotic behaviour as the single point $(\phi_\alpha, 0)$.*

Thus, if a trajectory starting from $(\phi_\alpha, 0)$ is attracted to a periodic orbit then so will all trajectories with initial conditions in $\mathscr{D}$ and its pre-iterates.

We now calculate the form taken by the pre-iterates of $\mathscr{D}$. The point $A_1 \in S^1 \cap W^1$ constructed in §3 has the pre-iterate $B_1 \in S^2 \cap (v = 0)$. By applying the results of §2 (*b*) we may deduce that B_1 has, in turn, the pre-iterate C_1 lying on the intersection of S^3 with S^1 and which is also a limit point of the set S^2. If we now compute the pre-image of that portion of S^2 lying between B_1 and A_2 we see that it forms a part of S^3 which intersects S^1 at the point C_1 and approaches S^1 again at the point C_2 which is the pre-image of B^2 such that $C_2 \in S^1 \cap S^4$. Indeed, S^3 forms a loop around the end-point of S^1 which is the pre-image of the point $(\phi_\beta, 0)$. Following the discussion in §2 it is evident that S^3 intersects S^1 tangentially at C_1 and approaches it transversally at C_2. A similar argument applied to the portion of S^n lying between B_{n-1} and A_n, shows that the pre-iterate of this set forms a loop around the end of S^1 intersecting it tangentially at C_{n-1} and approaching it at C_n. We illustrate this behaviour in figure 13.

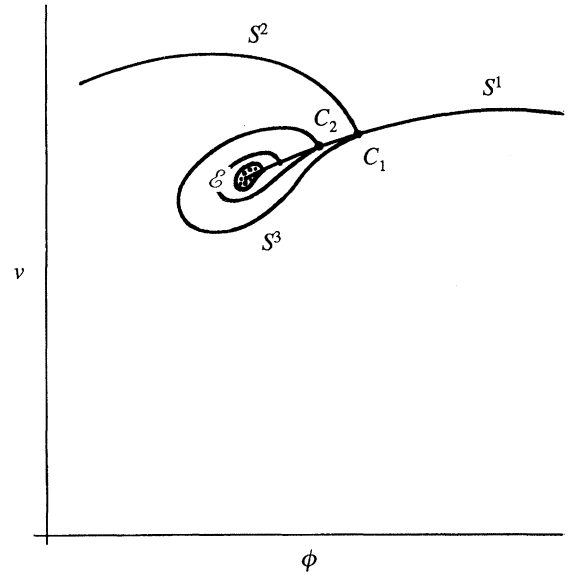

Figure 13. The region $\mathscr{E}$ surrounding the end-point of the set S^1 which is mapped into the region $\mathscr{D}$.

The resulting curves accumulate onto the pre-image of the portion of $\mathscr{C}$ which lies between B_∞ and A_∞. This curve loops around the endpoint of S^1 and intersects it twice at the point C_∞ which is the limit of the points C_n as $n \to \infty$. The loop encloses a non-empty region $\mathscr{E}$ containing the point $P^{-1}(\phi_\beta, 0)$ such that $P(\mathscr{E})$ is that subset of $\mathscr{D}$ bounded by $\mathscr{C}$, W^1 and the line $v = 0$. Any point in $\mathscr{E}$ will form an initial point of a trajectory with chatter. The pre-images of $\mathscr{E}$ are similarly non-empty regions containing the points $P^{-n}(\phi_\beta, 0)$. Any point in such a region is ultimately mapped into $\mathscr{D}$ and hence is attracted onto the same trajectory. We denote the union of these regions, together with $\mathscr{D}$, by $\mathscr{F}$, which is then the domain of attraction of the sticking region I. The general form of $\mathscr{F}$ is clearly visible in figure 10 and also in the domains of attraction of the two periodic attractors for P given when $\omega = 2.6$, $\sigma = 0$ which is presented in figure 4. In the latter example the set $\mathscr{F}$ is visible as a union of sets, each centred on the end points of a set S^n and all attracted to the $(6, 6)$ orbit.

We can extend our understanding of the domains of attraction of the fixed points of P by considering the asymptotic behaviour of the trajectories with incomplete chatter which have an initial point close to $\mathscr{C}$. As we have shown, $\mathscr{C}$ is an accumulation of the sets S^n and these sets lead to considerable stretching of the phase space. Consequently, we would expect that the domain of attraction will have a complex form close to $\mathscr{C}$. Our discussions in §2 showed that a set of data 'parallel' to a set S^n is not stretched by the action of P whereas a set of data which intersects S^n transversely is considerably stretched by P. This simple observation indicates that two points joined by a chord parallel to S^n are likely to have the same asymptotic behaviour and be mapped to the same attractor, whereas two points joined by a chord which intersects S^n may be mapped to different attractors. The resulting form of the domain of attraction of the two attractors given when $\omega = 2.6$, $\sigma = 0$ in a neighbourhood of $\mathscr{C}$ is illustrated schematically in figure 14 and takes the form of a series of 'stripes' roughly parallel to $\mathscr{C}$. The pre-iterates of this neighbourhood of $\mathscr{C}$ are in turn a series of stripes surrounding the various

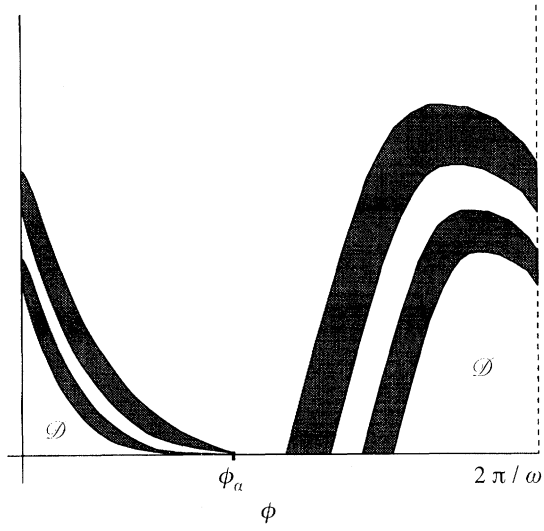

Figure 14. The 'striped' nature of the domain of attraction close to the region $\mathscr{D}$.

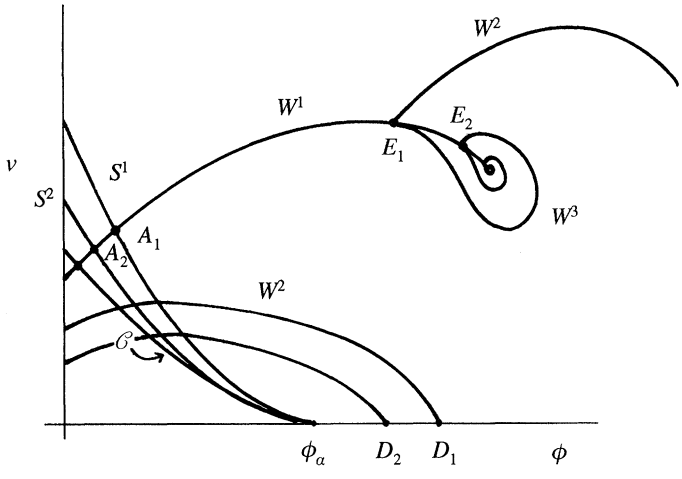

Figure 15. The accumulation of the sets W^n onto the end-point of the set W^1.

components of the set $\mathscr{F}$ which, by the arguments above, will form a series of loops around the end-points of the sets S^n. This short discussion explains the loops visible in figure 4 which are, in turn, the boundaries of the components of the set $\mathscr{F}$.

To see more precisely why this behaviour occurs, we consider the images of the sets V_n, defined to be the subsets of W^1 lying between the points A_n and A_{n+1} but not including the point A_{n+1}. A simple calculation shows that the set $P^m(V_n)$ is a subset of W^{m+1} that lies between S^{n-m} and S^{n-m+1} if $m < n$, and between S^1 and the line $\{v = 0\}$ if $m = n$, intersecting $\{v = 0\}$ at the point $D_n = P^n(A_n)$. Furthermore, the set $P^{n+1}(V_n)$ is a subset of W^{n+2} that intersects W^1 tangentially at the point $E_n = P^{n+1}(A_n)$, loops round the end point, E_∞, of W^1, given by $P((\phi_\alpha, 0))$, and approaches W^1 transversely at the point E_{n+1}. We illustrate this behaviour in figures 15 and 16. These figures are closely related to the strange attractors of various forms of chaotic behaviour and we shall return to this in the next section.

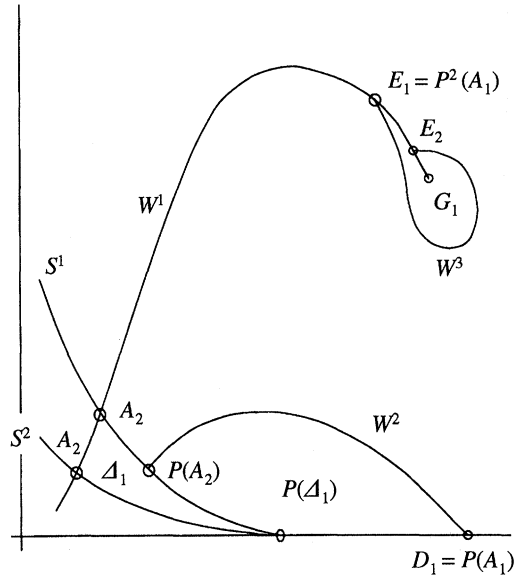

Figure 16. The approximately triangular set Δ_1 and two of its iterates.

The behaviour of these curves is very similar to that of the curves S^n close to the endpoint of S^1. However, there is a significant difference in that as $n \to \infty$,

$$D_n \to (\phi_\alpha, 0), \quad E_n \to P(\phi_\alpha, 0).$$

The approximately triangular region Δ_n, bounded by the sets V_n, S^n, S^{n+1} and the point $(\phi_\alpha, 0)$, is mapped by P^n onto the region bounded by $P^n(V_n)$, S^1 and the line $v = 0$ and by P^{n+1} onto the region G_n, on the end of W^1, that is bounded by the loop made by W^{n+2} and that part of W^1 lying between the points E_n and E_{n+1}. Furthermore, as $n \to \infty$ the sets G_n accumulate onto the single point E_∞.

The precise form of the domain of attraction of P close to $\mathscr{C}$, and for the pre-iterates of these points, is then determined by the form of this domain in a neighbourhood of the single point E_∞. If we consider the special case in which P has precisely two attracting states A and B, then in this case two possibilities may arise.

(i) E_∞ is interior to the domain of attraction of A (or B).

(ii) E_∞ is on the boundary of the domain of attraction of A (or B) (or, perhaps, is very close to the boundary).

In case (i) the sets G_n (which decrease in size as $n \to \infty$) will ultimately all lie inside the domain of attraction of A (or B). Consequently, close to $\mathscr{C}$, all trajectories will be attracted to A (or B). In contrast, in case (ii) the boundary of the domain of attraction of A (or B) will intersect G_n for all n and hence, some points of V_n will be attracted to A and some will be attracted to B. As a consequence each region V_n will contain 'stripes' which are attracted to A or B. This behaviour is illustrated in figure 17 and accounts for the structure observed in figure 14 and also in figure 4.

5. Periodic chatter and chaos

Finally we study the occurrence of trajectories in which chatter is repeated. Such trajectories are necessarily periodic. Closely related to these are chaotic trajectories with recurrent examples of interrupted chatter.

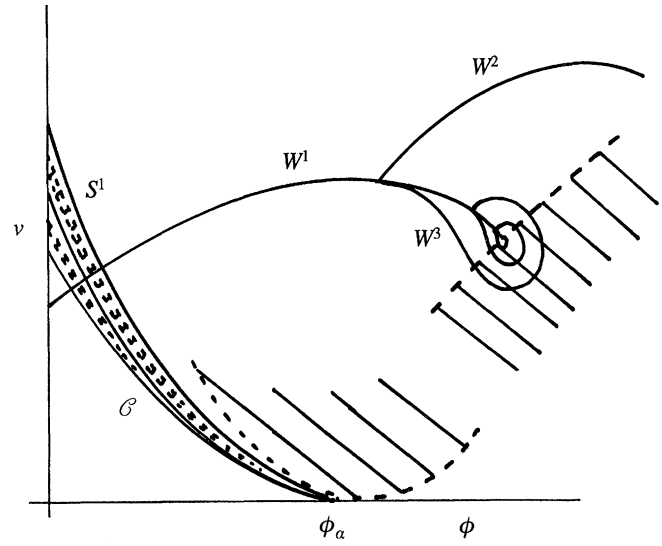

Figure 17. The intersection of the sets W^n with the domain of attraction of point A shown shaded and the resulting pre-iterates of this region.

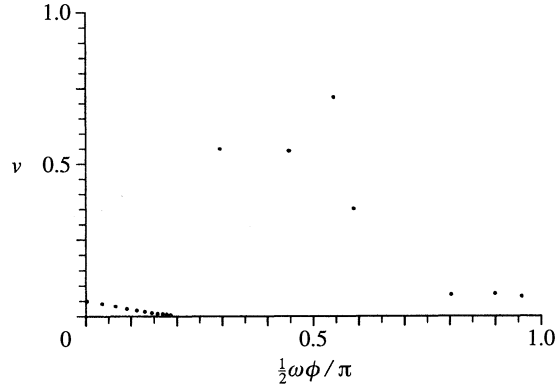

Figure 18. The sequence of points lying on the periodic orbit with chatter which occurs when $\omega = 2.7$ and $\sigma = 0$.

A trajectory with chatter necessarily evolves in subsequent time as the iterates $F^n = P^n(\phi_\alpha, 0)$ of the single point $(\phi_\alpha, 0)$. These iterates are also the 'end-points' of the sets W^n. Such a trajectory will be periodic if F^N lies inside $\mathscr{D}$ for some value of $N < \infty$ (or alternatively if $F^{N-1} \in \mathscr{E}$ etc.). As the sets $\mathscr{D}$ (and $\mathscr{E}$) have non-zero measure it is likely that this will occur for a range of values of the parameters r, ω and σ. For example, if σ and r are fixed then we would expect to see an interval of values $[\omega_1, \omega_2]$ at which periodic chatter is observed, such that at ω_1 and ω_2 then $F^N \in \mathscr{C}$ is on the boundary of $\mathscr{D}$, and for $\omega_1 < \omega < \omega_2$ then F^N lies inside $\mathscr{D}$. Indeed if $r = 0.8$ and $\sigma = 0$ then such an interval occurs for

$$2.692 < \omega < 2.701 \quad \text{and} \quad N = 5.$$

The resulting iterates F^n for the particular case $\omega = 2.7$ are illustrated in figure 18.

It follows, by construction, that if $\omega_1 < \omega < \omega_2$, then the end-point $E_\infty (= F^1)$ of W^1 must lie interior to the domain of attraction of the periodically chattering orbit.

Figure 19. The domain of attraction of the (2, 2) (shaded), (8, 6) (white) and periodically chattering (black) orbits that occur when $\omega = 2.7$ and $\sigma = 0$.

First, this implies that any such an orbit must be stable. Second the domain of attraction must then be of the form (i) described in §4. Indeed the domain of attraction for the periodically chattering orbit is rather large and is illustrated in figure 19.

We now suppose that ω is slightly greater than ω_2 so that F^N lies just outside $\mathscr{D}$. Instead of experiencing chatter the further iterates of F^N will form an incomplete chattering sequence. Indeed there will be a further point F^{N+M} such that $F^{N+M} \approx (\phi_\alpha, 0)$ and $F^{N+M+1} \approx F^1$. In this case F^{2N+M} will be close to F^N but, owing to the effects of stretching will be further away from $\mathscr{D}$ than F^N is. There will be a sequence of such points F^{3N+2M}, F^{4N+3M} etc. each giving an incomplete chattering sequence until the points are too far from $\mathscr{D}$ for incomplete chatter to be observed. This behaviour is illustrated in figure 20. The subsequent behaviour of the points F^k is then going to be very different from the chattering sequence and will probably be attracted to a very different asymptotic state. We conclude that the periodic chatter observed for $\omega \in [\omega_1, \omega_2]$ does not deform continuously into another form of periodic motion when ω leaves this interval but is likely to be replaced by a very different form of asymptotic state.

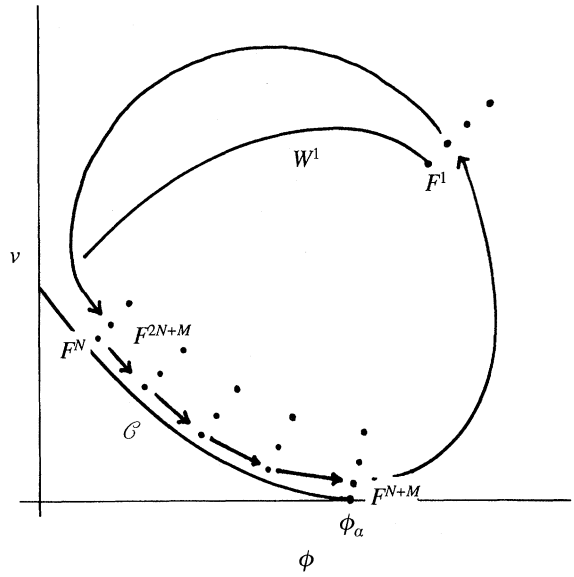

Figure 20. The sequence of iterations of the point $(\phi_\alpha, 0)$ when $\omega > \omega_2$.

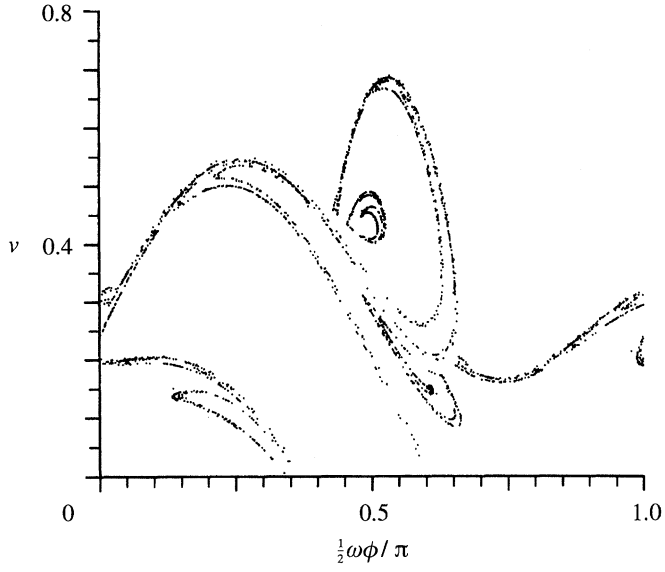

Figure 21. The strange attractor for the chaotic motion that arises when $\omega = 2.8$ and $\sigma = 0$.

Indeed, if we continue to consider the above example and let ω increase from 2.701, we find that the iterates of P have a chaotic behaviour. The strange attractor of this motion when $\omega = 2.8$ is illustrated in figure 21 (the corresponding trajectory is given in figure 2 (b)). Some of the structure of the strange attractor can be understood in terms of trajectories which include incomplete chatter. In particular it is shown in Whiston (1992) that the strange attractor of a chaotic orbit is, in general, close to the set $W_\infty \equiv \bigcup_{n=1}^{\infty} W^n$. Now, the analysis in the previous section, summarized in figure 15, showed that as a result of the intersection of W^1 with $\mathscr{C}$, the set W_∞ includes a series of loops connected to W^1 and accumulating on the point $P(\phi_\alpha, 0)$. Orbits

mapped onto these loops necessarily include sequences of interrupted chatter. Inspection of figure 21 shows that the strange attractor certainly inherits a great deal of the structure of W^{∞} with the loops close to the end point of W^{1} clearly visible. The related sequences of incomplete chatter are visible in figure 2(*c*). Very similar behaviour can be observed in the strange attractors of the chaotic trajectories of orbits with different parameter values and will occur in general whenever one of the iterates of the point $(\phi_{\alpha}, 0)$ lies close to the curve $\mathscr{C}$. For the case $\sigma = 0$ this occurs when ω is close to an odd integer and partly explains the fact that chaos is frequently observed for these values (see the discussions in Shaw & Holmes 1983; Budd *et al.* 1993).

6. Conclusions

We have shown that chatter can arise quite naturally in the idealized impact oscillator and that it helps explain both the forms of the domain of attraction of periodic attractors and the strange attractors of chaotic motions. The discussions in this paper have been of a rather idealized model, but it is significant that the set $\mathscr{D}$ calculated is large and will therefore be stable to perturbations of the model which make it more realistic. (Although we would have to modify the precise definition of chatter in the case of different impact laws.) As the dynamical significance of chatter is largely related to the interaction of $\mathscr{D}$ and its iterates with the set S^{1}, it is probable that some of the predictions of this paper are also true for more realistic models. We leave this as a subject for future investigation.

References

Budd, C. & Dux, F. 1994 Intermittency in an impact oscillator close to resonance. *Nonlinearity* (In the press.)

Budd, C., Cliffe, K. A. & Dux, F. 1993 The effect of frequency and clearance variations in single degree of freedom impact oscillators. Bristol University Report No. AM-93-02.

Foale, S. & Bishop, S. 1992 Dynamical complexities of forced impacting systems. *Phil. Trans. R. Soc. Lond.* A **338**, 547–555.

Goyda, H. & Teh, C. 1989 A study of the impact dynamics of loosely supported heat exchanger tubes. *J. Pressure Vessel Technol.* **111**, 394–401.

Katok, A. & Strelcyn, J.-M. 1980 Invariant manifolds, entropy and billiards: smooth maps with singularities. *Lecture Notes in Mathematics* **1222**. Springer-Verlag.

Nordmark, A. 1991 Non-periodic motion caused by grazing incidence in an impact oscillator. *J. Sound Vib.* **145**, 279–297.

Shaw, H. & Holmes, P. 1993 A periodically forced piecewise linear oscillator. *J. Sound Vib.* **90**, 129–155.

Thompson, J. & Stewart, H. 1986 *Nonlinear dynamics and chaos.* New York: John Wiley.

Whiston, G. 1992 Singularities in vibro-impact dynamics. *J. Sound Vib.* **152**, 427–460.